Cluster distribution in paraelectric KH_2AsO_4. II. ^{75}As spin-spin and spin-lattice relaxation

R. Blinc, M. Koren, J. Slak, V. Rutar, and S. Žumer
J. Stefan Institute, Department of Physics, E. Kardelj University of Ljubljana, 61000 Ljubljana, Yugoslavia

J. L. Bjorkstam
University of Washington, Seattle, Washington
(Received 13 November 1985)

The ^{75}As spin-lattice relaxation rate as well as the ^{75}As homogeneous and inhomogeneous linewidth has been measured in paraelectric KH_2AsO_4 as a function of temperature and orientation of the crystal in the external magnetic field. The results show that we are dealing (on the NMR time scale) with a continuous distribution of quasistatically polarized crystal regions ranging from zero local polarization to fully polarized states, which is symmetric as far as the sign of the polarization is concerned and strongly peaked at zero polarization. The distribution becomes broader and broader as the Curie temperature is approached from above.

I. INTRODUCTION

KH_2AsO_4 (KDA) is together with isomorphous KH_2PO_4 (KDP) a model substance[1] for the study of order-disorder transitions in H-bonded ferroelectrics. The soft-mode dynamics is here connected with the fast (10^{-11}–10^{-12} s) motion of protons between the two sites in the O—H $\cdots$ O bonds. It is basically determined by short-range Slater-Takagi rules,[2,3] which, to a certain extent, can be simulated by an Ising model in a transverse field Hamiltonian.[1,4,5]

In addition to the soft-mode motion, dynamic symmetry-breaking phenomena and local pseudo-freeze-out effects have been observed on the time scale of electron paramagnetic resonance (EPR) experiments ($\sim 10^{-7}$ s) in doped crystals,[6] and on the nuclear magnetic resonance (NMR) time scale in nominally pure crystals.[7–18]

Between $T_c = 96$ K and $T_c + 60$ K, anomalous ^{75}As NMR lines have been observed in KDA in addition to normal paraelectric lines.[7,10] These anomalous lines display the symmetry of the low-temperature ferroelectric phase well above T_c and arise from quasistatic polarized clusters[10] as demonstrated by electric field effects. The detailed nature of these clusters is not yet clear. They are insensitive to crystal annealing, in contrast to defects giving rise to the central peak observed in light scattering[12,13] but depend on crystal-growth conditions.[10]

The anomalous ^{75}As lines have recently been assigned[10] to four chemically equivalent but physically inequivalent As electric field gradient (EFG) tensors which have at $T = T_c + 1$ K, a quadrupole coupling constant $e^2 T_{ZZ} Q/h = 8.547$ MHz, and an asymmetry parameter $\eta = (T_{XX} - T_{YY})/T_{ZZ} = 0.35$. Their largest principal axis points along the fourfold crystal axes, $T_{ZZ} \| \mathbf{c}$, whereas the two minor principal axes are rotated with respect to the crystal a axis, $\angle(T_{XX}, \mathbf{a}) = \pm 26°$ and $\pm 64°$. These tensors are very different from the paraelectric electric-field-gradient (EFG) tensor[7,8] which is axially symmetric, $\eta = 0$, as well as the ferroelectric EFG tensors[1,8,14] where $e^2 T_{ZZ} Q/2h = 33.7$ MHz and $\eta \approx 0.55$. The anomalous ^{75}As EFG tensors[10] can be obtained in a straightforward way within the Slater model[1,2,7] if a small quasistatic spontaneous polarization, $p \neq 0$, is biasing the fast proton exchange within the six Slater H_2AsO_4 configurations.[7] Within the same model, the paraelectric EFG tensor is obtained if $p = 0$, whereas the ferroelectric EFG tensor corresponds to the situation where $p \approx 1$.

A study[15] of the frequency dependence of the proton spin-lattice relaxation time T_1 in paraelectric KH_2AsO_4 demonstrated the presence of a continuous distribution of partially polarized crystal regions which sharply increases at lower p values. The obtained results did not allow for a discrimination between a continuous distribution of quasistatically polarized clusters or a continuous polarization distribution within a given region centered around a defect. In order to check on the nature of this distribution at low p values (where the proton-As cross relaxation method fails because of too short a proton T_1) we decided to study the ^{75}As spin-lattice relaxation time in the laboratory and rotating frames as well as the homogeneous and inhomogeneous ^{75}As NMR linewidth.

II. EXPERIMENT

Our ^{75}As NMR data were obtained on the central $\frac{1}{2} \rightarrow -\frac{1}{2}$ transition at $\nu_L = 41$ MHz using a superconducting magnet and a Fourier-transform pulsed NMR spectrometer. The ^{75}As spin-lattice relaxation time T_1 was studied with a $\pi - \tau - \pi/2 - 80\ \mu s - \pi_{90°} - 80\ \mu s$ echo sequence. The width of the $\pi/2$ pulse was 10 μs. A spin-echo technique was also used to obtain the ^{75}As relaxation in the rotating frame, $T_{1\rho}$, and the spin-spin relaxation time T_2. The inhomogeneous ^{75}As linewidth was studied via the free-induction decay.

III. RESULTS

A. ^{75}As linewidth

The temperature dependence of the ^{75}As spin-spin relaxation time T_2 is given in Fig. 1. On cooling below room temperature at $\mathbf{c}\perp\mathbf{H}_0$, $\angle(\mathbf{a},\mathbf{H}_0)=30°$, T_2 initially increases slightly from ~ 130 to ~ 150 μs and then decreases to ~ 105 μs on approaching T_c. As can be seen from the inset in Fig. 1, T_2 only slightly varies with angle for $\mathbf{c}\perp\mathbf{H}_0$ even at $T=T_c+1.5$ K. The inhomogeneous linewidth (Fig. 4)—as determined from the free-induction decay—is of the order of T_2 far from T_c but in contrast to T_2 sharply increases on cooling towards T_c (Fig. 1). Close to T_c, the inhomogeneous linewidth $\Delta\nu$ becomes much larger than the homogeneous one. The angular variation of $\Delta\nu$ for the rotation around the c axis (inset to Fig. 1) is much stronger than the angular variation of T_2 and becomes more and more pronounced as $T\rightarrow T_c$ in agreement with the data of Ref. 14. The inhomogeneous linewidth of the $\frac{1}{2}\rightarrow-\frac{1}{2}$ transition is symmetric with respect to $\theta_c=45°$—where θ_c is the angle between H_0 and the a axis for $c\perp\mathbf{H}_0$—and repeats every 90°. At all temperatures, the linewidth is smallest for $\theta_c=18.5°$ where the static magnetic field bisects the angle between the upper and lower O $\cdots$ O bond directions (Fig. 4b). The shape of the free-induction decay is neither Gaussian nor Lorentzian (Fig. 2) and strongly varies with temperature.

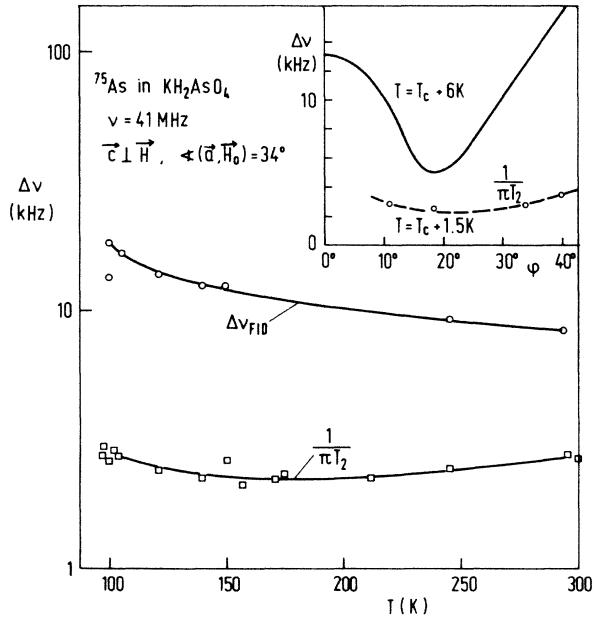

FIG. 1. Temperature dependence of the ^{75}As $\frac{1}{2}\rightarrow-\frac{1}{2}$ spin-spin relaxation rate T_2^{-1} as determined from a spin-echo sequence and the inhomogeneous linewidth $\Delta\nu$ determined from the free-induction decay (FID). The inset shows the angular variation of the homogeneous linewidth $(\pi T_2)^{-1}$ and the inhomogeneous one $\Delta\nu$.

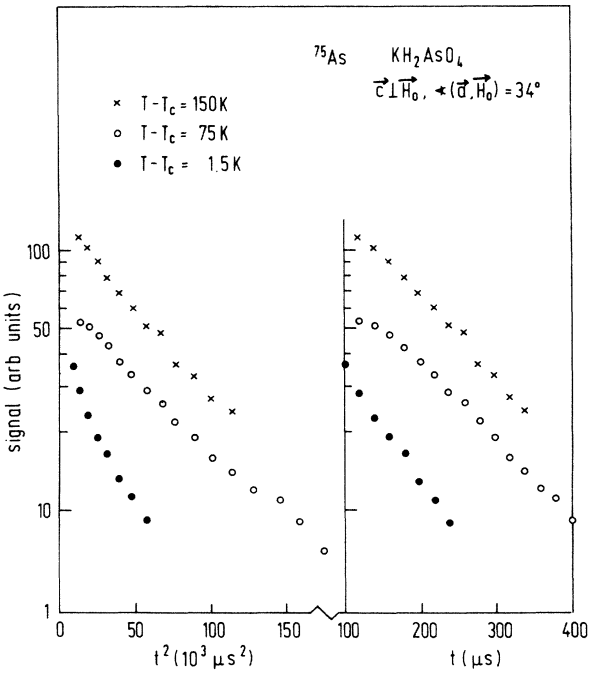

FIG. 2. Plot of the logarithm of the free-induction decay signal versus t^2 and t. The results show that the inhomogeneous linewidth is neither Gaussian nor Lorentzian.

B. ^{75}As spin-lattice relaxation

The temperature dependences of the ^{75}As spin-lattice relaxation times T_1 and $T_{1\rho}$ are presented in Fig. 3. T_1 is rather short, $200\ \mu s\leq T_1\leq 400\ \mu s$, and about 2–3 times longer than T_2. It initially increases and then decreases with decreasing temperature between 273 K and T_c. Its angular variation is more pronounced than the angular variation of T_2 (inset, Fig. 3). $T_{1\rho}$ is intermediate between T_1 and T_2.

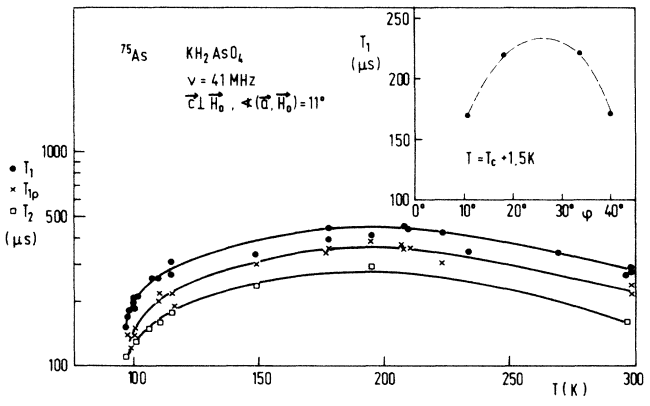

FIG. 3. Temperature dependence of the ^{75}As spin-lattice relaxation time in the laboratory (T_1) and rotating frames ($T_{1\rho}$). The temperature dependence of T_2 is shown for comparison. The inset shows the angular dependence of T_1.

IV. THEORY

A. ^{75}As EFG tensors

The EFG tensor at the As site in KDA is of covalent nature and its instantaneous value depends on the arrangement of the four protons around a given AsO_4 group:

$$T=T(p_1,p_2,p_3,p_4)\ , \tag{1}$$

where p_i is the instantaneous value of the local order parameter for the ith O—H $\cdots$ O bond. The variation of T with time is thus determined by the time variation of $p_i(t)$, i.e., by the motion of hydrogens between the two equilibrium sites in each of the four hydrogen bonds surrounding a given AsO_4 group.

Expanding $T(t)$ in terms of $p_i(t)$ up to second-order terms we get

$$T(t)=T_0+\sum_i A_i p_i+\sum_{\substack{i,j\\ i<j}} B_{ij}p_i p_j+\cdots\ . \tag{2}$$

Introducing, as was done in the preceding paper,[15]

$$p_i(t)=p+\Delta p_i(t)\ , \tag{3a}$$

where

$$\langle p_i\rangle=\langle p_j\rangle=p \tag{3b}$$

stands for the average polarization of a given cluster, we get for the time-average EFG tensor,

$$\langle T(t)\rangle=\begin{cases} T_0+\sum\limits_{\substack{i,j\\ i<j}} B_{ij}\langle \Delta p_i\Delta p_j\rangle+\cdots\ , & p=0 \quad (4a)\\ T_0+Ap+Bp^2+\cdots\ , & p\neq 0\ . \quad (4b)\end{cases}$$

For the equilibrium situation in a homogeneous crystal, $p=0$ for $T>T_c$ and $p\neq 0$ for $T<T_c$.

Here $A=\sum_i A_i, B=\sum_{i<j}B_{ij}$ and we have from point-symmetry considerations in the AsO_4 fixed x,y,z frame:[8,18]

$$T_0=t\begin{bmatrix}1&0&0\\0&1&0\\0&0&-2\end{bmatrix},\quad B=b\begin{bmatrix}1&0&0\\0&1&0\\0&0&-2\end{bmatrix},$$
$$A=a\begin{bmatrix}-1&0&0\\0&1&0\\0&0&0\end{bmatrix}, \tag{5}$$

where $a>t>b$. It should be noted that here $p=1$ corresponds to a state where two protons are "close" to the upper oxygen atoms of a given AsO_4 group and two protons are "far" from the lower oxygen atoms of the same group, whereas $p=-1$ corresponds to a reversal of the protonic configurations.

Above T_c the largest principal axis of the EFG tensor T_{ZZ} points along the z||c axis and the EFG tensor is axially symmetrical, $\eta=0$. The presence of a nonzero p value destroys the cylindrical symmetry of the EFG tensor thus producing a nonzero value of the asymmetry parameter η. For large p values T_{ZZ} points—depending on the sign of p—along the upper or lower O $\cdots$ O direction of the AsO_4 group (i.e., along x or y) rather than along z.

B. ^{75}As spin-lattice relaxation

Whereas the ^{75}As quadrupole perturbed NMR spectra are determined by the time-averaged value of the total spin Hamiltonian

$$\mathcal{H}=\mathcal{H}_Z+\mathcal{H}_Q+\mathcal{H}_D\ , \tag{6a}$$

where $\mathcal{H}_Z$ stands for the Zeeman, $\mathcal{H}_Q$ for the quadrupole and $\mathcal{H}_D$ for the dipole-dipole part, the ^{75}As spin-lattice relaxation rate depends on the spectral density of the autocorrelation function of the matrix elements of the fluctuating part[18] of the Hamiltonian:

$$\mathcal{H}_1(t)=\mathcal{H}-\langle\mathcal{H}\rangle\approx\mathcal{H}_Q-\langle\mathcal{H}_Q\rangle$$
$$=E\sum_l\sum_{k=-2}^{+2} D_l^{(-k)}\Delta T_l^{(k)}\ , \tag{6b}$$

taken with respect to the eigenfunctions of $\langle\mathcal{H}\rangle$. Assuming that the linear terms in $p_i(t)$ and p in (2) and (4b) are dominant, one can write the rapidly fluctuating part of the EFG tensor (governed by the proton motion in the soft mode) in the crystal fixed frame as:

$$\Delta T_s=\tfrac{1}{4}A\sum_{i=1}^{4}\Delta p_i(t)\ . \tag{7}$$

Let us further assume that the cluster polarization p biasing the proton motion is quasistatic above T_c and slowly changes with time. The slowly fluctuating part of the EFG tensor can then be expressed in the crystal fixed frame as

$$\Delta T_p=\tfrac{1}{4}Ap(t)\ . \tag{8}$$

In the eigenframe of $\langle\mathcal{H}\rangle$ we can express (7) and (8) as

$$V_s(t)=S\Delta T_s S^{-1} \tag{9a}$$

and

$$V_p(t)=S\Delta T_p S^{-1}\ , \tag{9b}$$

where S is the matrix transforming the AsO_4 fixed frame into the magnetic field fixed laboratory frame. Introducing $\tilde{A}=SAS^{-1}$ we obtain the corresponding spectral densities as

$$J_s^{(k)}(k\omega)=\int_{-\infty}^{+\infty}\langle V_s^{(k)}(0)[V_s^{(k)}(t)]^*\rangle e^{ik\omega t}dt$$
$$=|\tilde{A}^{(k)}|^2 j_s^{(k)}(k\omega)\ , \tag{10a}$$

where

$$\tilde{A}^{(0)}=\tilde{A}_{zz},\quad \tilde{A}^{(\pm1)}=\tilde{A}_{xz}\pm i\tilde{A}_{yz}\ ,$$

and

$$\tilde{A}^{(\pm2)}=\tfrac{1}{2}\tilde{A}_{xx}-\tilde{A}_{yy}\pm i\tilde{A}_{xy}$$

and

$$j_s^{(k)}(k\omega)=\tfrac{1}{16}\sum_{i,j=1}^{4}\int_{-\infty}^{+\infty}\langle\Delta p_i(0)\Delta p_j(t)\rangle e^{ik\omega t}dt\ , \tag{10b}$$

and

$$J_p^{(k)}(\omega)=|\tilde{A}^{(k)}|^2 j_p(k\omega)\ , \tag{11}$$

with

$$j_p(\omega)\approx\frac{2p^2\tau_p}{1+(\omega\tau_p)^2}\ , \tag{12}$$

and with τ_p standing for the cluster lifetime and p for the average cluster polarization. Making use of the dynamic Ising model and the fluctuation-dissipation theorem, one can express[16] $j_s(\omega)$ in the fast motion limit $\omega\tau\ll 1$ as

$$j_s(\omega)=(1-p^2)I(T,p)\tau\ , \tag{13}$$

where τ is the proton O—H $\cdots$ O bond reorientation time in the absence of interactions and

$$I(T,p)=\frac{1}{8}\frac{1}{N}\sum_q\sum_{i,j=1}^{4}e^{i\mathbf{q}\cdot(\mathbf{r}_i-\mathbf{r}_j)}\times\left[\frac{T}{T-T_c(q)(1-p^2)}\right]^2\ , \tag{14}$$

with $T_c(\mathbf{q})=J(\mathbf{q})/k$ standing for the Fourier transform of the Ising model interaction constant known from neutron scattering experiments.[17] For $T>T_c$, the number of clusters with $p>0.1$ is small[15] so that their influence on $I(T,p)$ can be neglected.

Therefore we can take $p=0$ in evaluating expression (14). We then find for $\omega\tau\ll 1$ the soft-mode contribution as

$$j_s(\omega)=I(T)\tau=j_s(0)\ . \tag{15}$$

On the NMR time scale, τ_p is expected to be long so that $\omega\tau_p\gg 1$ and the slowly fluctuating cluster contribution becomes

$$j_p(\omega)=2p^2/(\omega^2\tau_p)\ . \tag{16}$$

Using

$$\tilde{A}=a\begin{bmatrix}0 & 0 & 0\\ 0 & \cos(2\theta) & \sin(2\theta)\\ 0 & \sin(2\theta) & \cos(2\theta)\end{bmatrix}\ , \tag{17}$$

one finds for the total spectral density $J^{(k)}(\omega)=J_s^{(k)}(\omega)+J_p^{(k)}(\omega)$

$$J^{(0)}(0)=\tfrac{1}{2}a^2[1+\cos(4\vartheta)][j_s(0)+j_p(0)]\ , \tag{18a}$$

$$J^{(1)}(\omega)=\tfrac{1}{2}a^2[1-\sin(4\vartheta)][j_s(0)+j_p(\omega)]\ , \tag{18b}$$

$$J^{(2)}(\omega)=\tfrac{1}{8}a^2[1+\cos(4\vartheta)][j_s(0)+j_p(\omega)]\ , \tag{18c}$$

where $e^2Qa/h=33.7$ MHz and ϑ is the angle between H_0 and the direction of the largest principal axis of the fluctuating EFG tensor.

In the case of unequally spaced quadrupole perturbed ^{75}As Zeeman energy levels, the approach of the magnetization to equilibrium will be multiexponential. This case was evaluated in Appendix A of Ref. 18.

Since for $T>T_c$ the average As NQR frequency ν_Q is much smaller than the As Zeeman frequency, $\nu_Q\ll\nu_L$, we have

$$T_1^{-1}\approx W^{(1)}+W^{(2)}\ , \tag{19a}$$

where the two-spin transition probabilities are

$$W^{(1)}=\frac{e^4Q^2}{12\hbar^2}J^{(1)}(\omega) \tag{19b}$$

and

$$W^{(2)}=\frac{e^4Q^2}{12\hbar^2}J^{(2)}(2\omega)\ , \tag{19c}$$

and where

$$W^{(1)}\approx W^{(2)}\approx(3\times10^{15}\ \mathrm{s}^{-2})[I(T)\tau+p^2/(\omega^2\tau_p)] \tag{20}$$

for $\theta\approx 7.5°$.

For $p<0.1$, $\omega\sim 2.4\times10^8\ \mathrm{s}^{-1}$, and $\tau_p\gg10^{-6}$ s, the second term in expression (20) can be neglected in comparison with the first one. The measured ^{75}As spin-lattice relaxation rate—which represents the contribution of unpolarized or weakly polarized clusters—should thus be governed by the soft-mode contribution. The contribution of the polarized regions could be detected only if measured directly at the ^{75}As resonance frequency of nuclei in the polarized regions where $\nu_{Q,\mathrm{pol}}\gg\nu_Q$ and where the soft-mode contribution is reduced because of the $(1-p^2)$ factor.[1]

C. ^{75}As spin-spin relaxation and the homogeneous linewidth

The spin-spin relaxation rate T_2^{-1} for the transition $m\rightarrow m-1$ is given by

$$\frac{1}{T_2}=\frac{1}{T_2'}+\frac{1}{2}\left[\frac{1}{t_m}+\frac{1}{t_{m-1}}\right]\ , \tag{21}$$

where

$$\frac{1}{T_2'}=\int_{-\infty}^{+\infty}\langle\omega(0)\omega(t)\rangle dt\propto J^{(0)}(0) \tag{22}$$

is the adiabatic linewidth and the $1/t_m$ terms

$$\frac{1}{t_m}=\sum_m W_{m,m_i} \tag{23a}$$

with

$$W_{m,m_i}=\int_{-\infty}^{+\infty}e^{i\omega_{m,m_i}t}\langle\langle m\,|\,\mathscr{H}_1(0)\,|\,m_i\rangle\times\langle m_i\,|\,\mathscr{H}_1(t)\,|\,m\rangle\rangle dt \tag{23b}$$

take account of the lifetime broadening due to spin transitions $m\rightarrow m_i$. Here,

$$\hbar\omega=\langle m\,|\,\mathscr{H}_1(t)\,|\,m\rangle-\langle m-1\,|\,\mathscr{H}_1(t)\,|\,m-1\rangle\ , \tag{24}$$

where $\mathscr{H}_1(t)$ is given by expression (6b) and $|\,m\rangle$ are the eigenstates of $\mathscr{H}_Z+\langle\mathscr{H}_Q\rangle$.

Let us first assume that $\nu_L\gg\nu_Q$ so that $\langle\mathscr{H}\rangle\approx\mathscr{H}_Z$. In this case, one finds that the adiabatic linewidth of the $\frac{1}{2}\rightarrow-\frac{1}{2}$ transition

$$\frac{1}{T_2'(\frac{1}{2}\rightarrow-\frac{1}{2})}=\frac{e^4Q^2}{144\hbar^2}\,|\langle\tfrac{1}{2}|D^{(0)}|\tfrac{1}{2}\rangle-\langle-\tfrac{1}{2}|D^{(0)}|-\tfrac{1}{2}\rangle|^2\int_{-\infty}^{+\infty}\langle\Delta T^{(0)}(0)\Delta T^{(0)}(t)\rangle dt=0,\quad \nu_Q\rightarrow 0 \tag{25a}$$

vanishes as the quadrupolar Hamiltonian has no nonzero matrix elements connecting the $\frac{1}{2}\rightarrow-\frac{1}{2}$ states. The lifetime broadening yields

$$t_{1/2,-1/2}^{-1}=W_{1/2,3/2}+W_{1/2,-3/2} \tag{25b}$$

so that

$$T_2^{-1}(\tfrac{1}{2}\rightarrow-\tfrac{1}{2})=(e^4Q^2/12\hbar^2)\times[J^{(1)}(\omega)+J^{(2)}(2\omega)]\,, \tag{25c}$$

and the homogeneous linewidth of the $\frac{1}{2}\rightarrow-\frac{1}{2}$ transition should be determined by the spin-lattice relaxation rate,

$$T_2(\tfrac{1}{2}\rightarrow-\tfrac{1}{2})\approx T_1\,. \tag{25d}$$

For the $\frac{3}{2}\rightarrow\frac{1}{2}$ transition, one finds in the same approximation a nonzero adiabatic linewidth

$$\frac{1}{T_2'(\frac{1}{2}\rightarrow\frac{3}{2})}=\frac{e^4Q^2}{4\hbar^2}J^{(0)}(0)\,, \tag{25e}$$

so that

$$T_2^{-1}(\tfrac{1}{2}\rightarrow\tfrac{3}{2})=\frac{e^4Q^2}{4\hbar^2}[J^{(0)}(0)+\tfrac{1}{3}J^{(1)}(\omega)+\tfrac{1}{3}J^{(2)}(2\omega)] \tag{25f}$$

and the satellite linewidth should be different from T_1^{-1} and larger than the width of the central line if $J(0)>J(\omega)$ or $j(2\omega)$.

If $J(0)$ is significantly larger than $J(\omega)$, i.e., if there is a large central peak in the spectrum, the approximation $\langle\mathscr{H}\rangle\approx\mathscr{H}_Z$ is not good enough and one should take into account the quadrupole perturbation of the Zeeman eigenstates, i.e., $\langle\mathscr{H}\rangle\approx\mathscr{H}_Z+\langle\mathscr{H}_Q\rangle$. Using second-order perturbation theory, one now finds a small but nonzero value for the adiabatic width of the $\frac{1}{2}\rightarrow-\frac{1}{2}$ transition:

$$T_2^{-1}(\tfrac{1}{2}\rightarrow-\tfrac{1}{2})\approx\xi^2\frac{4e^4Q^2}{3\hbar^2}J^{(2)}(0)\,, \tag{25g}$$

where $\xi=\nu_Q/\nu_L\ll 1$. We thus see that the result $T_2(\frac{1}{2}\rightarrow-\frac{1}{2})<T_1$ implies that $J^{(2)}(0)>J(\omega)$, i.e., it implies the existence of a low-frequency motion in addition to the soft-mode motion. Even a large central peak will, however, only weakly affect T_2 of the central $\frac{1}{2}\rightarrow-\frac{1}{2}$ transition as long as $\nu_Q\ll\nu_L$ and $\xi^2\ll 1$.

D. ^{75}As inhomogeneous linewidth

The large difference between the homogeneous linewidth $\Delta\nu_h\approx 1/(\pi T_2)$ observed via the spin-echo sequence and the inhomogeneous linewidth $\Delta\nu$ observed via the free-induction decay suggests the presence of an anomalous anisotropic line broadening mechanism which becomes stronger on approaching T_c from above.

The variation of the inhomogeneous linewidth with temperature and crystal orientation in the external magnetic field can be explained as a superposition of second-order shifted-central $\frac{1}{2}\rightarrow-\frac{1}{2}$ ^{75}As lines corresponding to differently polarized clusters.

For $p=0$, the effective EFG tensor will be axially symmetric above T_c and the largest principal axis will point along the $z(c)$ direction. For $p\neq 0$, the cylindrical symmetry around the $z(c)$ axis will be destroyed.[8,18] In fully polarized clusters the smallest principal axis of the EFG tensor—corresponding to T_{XX}—is colinear with the crystal $z(c)$ axis and T_{ZZ} and T_{YY} are along the upper and lower O $\cdots$ O direction of the AsO_4 tetrahedra (Fig. 4). The T_{ZZ} and T_{YY} principal axes change position if the two protons attached to the AsO_4 group in the fully polarized state change from $+p$ to $-p$, i.e., if instead of the two protons being attached to the "upper" corners of the AsO_4 group, they become attached to the "lower" corners corresponding to a change in the direction of the spontaneous polarization. Finally, one should note that there are two differently oriented AsO_4 tetrahedra in the unit cell. The bisectors of the upper and lower O $\cdots$ O directions make an angle of $\pm 18.5°$ with the crystal **x** (**a**) axis.

For a given AsO_4 group in a cluster with a quasistatic polarization p we can now express the second-order quadrupolar shift of the central $\frac{1}{2}\rightarrow-\frac{1}{2}$ ^{75}As transition for a **c** rotation ($\mathbf{H}_0\perp\mathbf{c}$) as:

$$\nu_c^{(2)}(p)=K\{K_1+K_2\cos(2\varphi_c)p+[(K_3+K_4\cos(4\varphi_c)]p^2\}\,, \tag{26}$$

where $\varphi_c=\theta_c\pm 26.5°$ for the two differently oriented H_2AsO_4 tetrahedra and $\varphi_c\rightarrow\varphi_c\pm 90°$ if the polarization changes from $+p$ to $-p$. The coefficients K and $K_i, i=1-4$, depend on T_{ZZ}, T_{YY}, T_{XX}, and the Larmor frequency ν_L and are listed in the text to Fig. 5. The cluster polarization p is a function of temperature.

The observed line shape $F(\nu)$ now reflects the distribution $f(\nu)$ of second-order quadrupolar shifts $\nu_c^{(2)}$ resulting from a distribution of differently polarized regions $g(p)$ and of course also depends on the shape of the individual homogeneous lines which is assumed to be Gaussian with a root-mean-square width σ. Thus

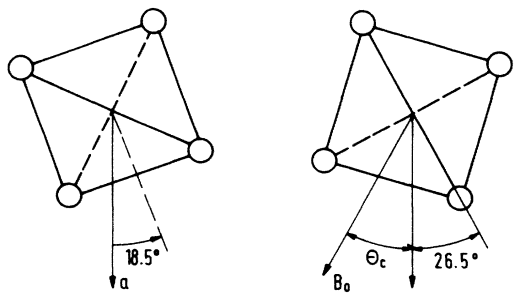

FIG. 4. The arrangement of the two physically nonequivalent AsO_4 tetrahedra in the paraelectric unit cell.

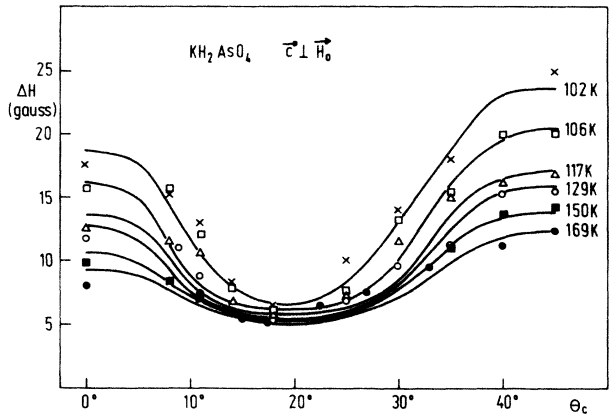

FIG. 5. Comparison between experimental and theoretical (——) angular dependences of the width of the ^{75}As $\frac{1}{2}\rightarrow-\frac{1}{2}$ NMR line according to equation (27). The values of the coefficients $K=0.405$ MHz, $K_1=0.228$, $K_2=2.11$, $K_3=17.08$, and $K_4=21.98$ were obtained from the measured As EFG tensors in the low-temperature ferroelectric phase (1,8,16,18), whereas $\bar{\sigma}=5\times10^{-3}$ was obtained from the high-temperature data.

$$F(\tilde{\nu})=\sum_{i=1}^{4}\int_0^{\infty} g(p)\exp\{-[\tilde{\nu}-\tilde{\nu}_{c,i}^{(2)}(p)]^2/2\tilde{\sigma}^2\}dp\ , \qquad (27)$$

where $g(p)$ is the normalized distribution of cluster polarizations, $\int_0^{\infty} g(p)dp=1$, $\tilde{\nu}_{c,i}^{(2)}=\nu_{c,i}^{(2)}/K-K_1$, $\tilde{\nu}=\nu/K-K_1$, $\bar{\sigma}=\sigma/K=5\times10^{-3}$ is the homogeneous linewidth (2 kHz), and the index i corresponds to the taking into account of the two differently oriented AsO_4 tetrahedra ($\varphi_c=\theta_c\pm26.5°$) and the two signs of the polarization: $\varphi_c\rightarrow\varphi_c\pm90°$. We assumed that clusters with $+p$ and $-p$ are equally probable on the time average.

It should be noted that Eq. (27) is equivalent to using

$$f(\nu)d\nu=g(p)dp\ , \qquad (28)$$

and convoluting the distribution of second-order quadrupolar shifts with the Gaussian function $L(\nu-\nu_i')$ describing the shape of the individual homogeneous lines

$$F(\nu)=\sum_{i=1}^{4}\int f(\nu_i')L(\nu-\nu_i')d\nu_i'\ . \qquad (29)$$

The computed angular dependence of the halfwidth of $F(\tilde{\nu})$ according to Eq. (27) is compared with the experimental data in Fig. 5. The agreement is satisfactory in view of the rather large scattering of the experimental points obtained in this and other[8,14] laboratories. A full discussion of the electric-field effects and the detailed comparison of the experimental and theoretical line shapes is reserved for a subsequent paper. We would just like to mention that the "paraelectric" A line observed by Mali *et al.*[10] corresponds to $p=0$ so that $\nu_c^{(2)}=KK_1\neq f(\varphi_c)$, whereas the angularly dependent "symmetry breaking" B lines can be explained by the presence of nuclei in crystal regions where the local quasistatic polarization is continuously distributed between zero and the full polarization.

V. DISCUSSION

The spin-lattice relaxation rate T_1^{-1} of the paraelectric (i.e., $\eta=0$) central ^{75}As $\frac{1}{2}\rightarrow-\frac{1}{2}$ line is dominated by two contributions: A contribution from slow, $\omega_L\tau\gg1$, hindered rotation of the H_2AsO_4 groups which at 41 MHz dominates T_1^{-1} above -80°C, and a "soft-mode" (SM) contribution, $(T_1^{-1})_{SM}\approx(6\times10^{15}s^{-2})I(T)\tau$, which dominates T_1^{-1} between -80°C and T_c and where $\omega_L\tau\ll1$. The contribution from hindered rotations of the H_2AsO_4 groups is similar to the ones found in other members of the KDP family and the same is true for the soft-mode contribution. The soft-mode T_1^{-1} anomaly in the fast motion regime is of logarithmic[1] nature, $T_1^{-1}\propto\ln(T-T_c)/T_c$, as expected for an anisotropic[16,17] $J(q)$ and the noninteracting proton intrabond reorientation time equals $\tau\approx0.3\times10^{-12}$ s. This time is short enough to allow for fast averaging over the various Slater H_2AsO_4 configurations.[1] The quasistatic polarization fluctuation contribution to the T_1 of the paraelectric line is negligible in comparison with the soft-mode contribution. This is expected, on the basis of Eq. (20), as the soft-mode relaxation mechanism is extremely effective. The fact that $T_{1\rho}$ is only slightly shorter than T_1 and that the line shape is not Lorentzian agrees with this interpretation and excludes the model proposed by Adriaenssens.[9]

The huge difference between the homogeneous and the inhomogeneous linewidth clearly demonstrates the presence of locally polarized quasistatic crystal regions which produce a polarization dependent shift of the As $\frac{1}{2}\rightarrow-\frac{1}{2}$ line. The angular and temperature dependence of the inhomogeneous linewidth can be quantitatively reproduced by Eqs. (26) and (27) (Figs. 5,6) implying a T-dependent continuous distribution of the local polarizations $g(p)$ in agreement with the proton-^{75}As cross-relaxation data.[15]

The local polarization distribution deduced from the

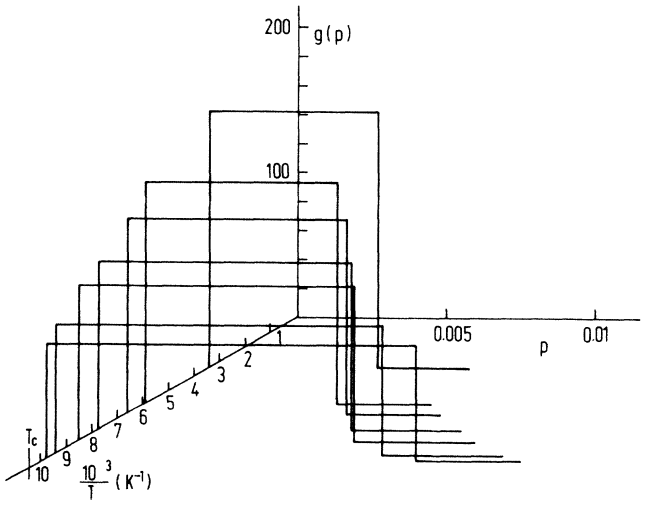

FIG. 6. Local quasistatic polarization fluctuation distribution obtained from the fit of the angular dependence of the ^{75}As $\frac{1}{2}\rightarrow-\frac{1}{2}$ half-width. The weak "high polarization" tail of $g(p)$ observed by the proton-As cross-relaxation technique is neglected.

linewidth data ranges from $p=-1$ to $p=1$ but the distribution $g(p)$ is sharply peaked at $p=0$ for $T>T_c$. In view of the shape of the $g(p)$ distribution, the linewidth is mainly determined by regions with small p values ($|p|<10^{-2}$), whereas the As-H cross-relaxation data yield reliable information mainly on regions with large p values ($|p|>10^{-1}$). For $|p|<10^{-2}$, $g(p)$ can be approximated by a square-shaped model

$$g(p)=\begin{cases}\text{const}, & |p|<p_0 \quad (30)\\ 0, & |p|>p_0 \quad (31)\end{cases}$$

or by a Gaussian. The square-shaped model gives a somewhat better fit at low-p values. The high polarization tail of $g(p)$ observed by the H-As cross-relaxation data is neglected here. The root-mean-square second moment of the square-shaped distribution is rather small. It sharply increases with approaching T_c from above (Fig. 7) and amounts at $T=T_c+1$ K to $\sigma_p=0.02$.

The two informations—from linewidth and H-As cross relaxation data—are thus complementary but there is a region $10^{-2}<p<10^{-1}$ where no reliable information on $g(p)$ is available as of yet. The detailed form of the distribution $g(p)$ therefore cannot be reliably determined from the present data.

The question whether the local polarization p is completely static or whether it slowly fluctuates in time cannot be definitely answered as of yet. The observed difference between T_1 and T_2 seems to demonstrate the presence of ultraslow motion which could be due to fluctuating cluster polarizations.

The results of this study together with the ^{75}As-proton cross-relaxation data are as follows:

(i) We confirmed the results of Mali *et al.*[10] concerning the quasistatic nature of the weakly polarized clusters in KDA in contrast to the Adriaenssens model.[9] The protons within the cluster are, however, moving between the two possible sites in the H bonds fast on the NMR time scale. Their motion is biased by the quasistatic cluster polarization.

(ii) We showed that we are in fact dealing with a continuous distribution of local polarization, ranging from $p=0$ to $|p|=1$.

(iii) We showed that the distribution is symmetric as far as the sign of p is concerned and strongly peaked at $p=0$.

(iv) We showed that the distribution becomes broader and broader in p as T_c is approached from above.

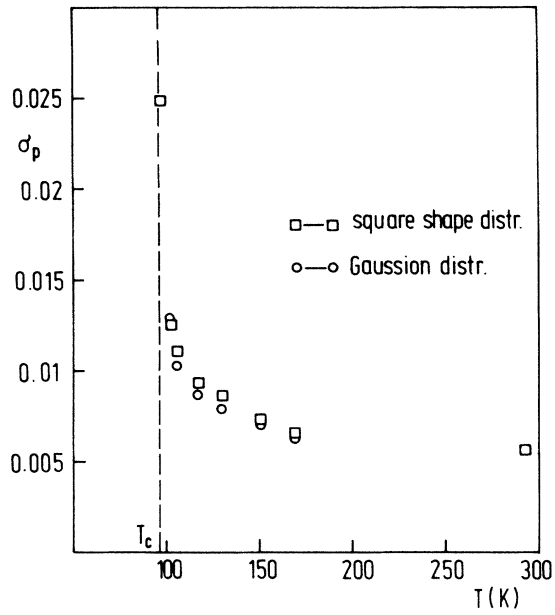

FIG. 7. Temperature dependence of the second moment of the local polarization distribution function $g(p)$.

(v) There are strong indications that the local polarization is slowly fluctuating with a correlation time which is at $T=T_c+2$ K of the order of the one found by dielectric dispersion data,[19,20] i.e., of the order of 30 ms.

(vi) The above data cannot definitely discriminate between a continuous distribution of clusters with different fractional local polarization or between a continuous polarization distribution within a given cluster which could be induced by charged defects.

Finally, it should be pointed out that the above phenomena observed in KDA are certainly not restricted to this crystal alone. They should occur in other order-disorder type H-bonded crystals as well. The reason that they are observed in KDA so clearly is the extremely high resolution of the ^{75}As quadrupole perturbed NMR spectroscopy. This is due to the large value of the As quadrupole coupling constant $e^2T_{ZZ}Q/h$ in the ferroelectric phase and the small value of $e^2T_{ZZ}Q/h$ in the paraelectric phase thus allowing for a clear observation of frequency shifts induced by even small local quasistatic polarization fluctuations with p of the order of only a few percent.

[1]For a review see, for instance, R. Blinc and B. Žekš, *Soft Modes in Ferroelectrics and Antiferroelectrics* (North-Holland, Amsterdam, 1974).

[2]J. C. Slater, J. Chem. Phys. **9**, 16 (1941).

[3]H. B. Silsbee, E. A. Uehling, and V. H. Schmidt, Phys. Rev. **133**, A165 (1964); R. Blinc and S. Svetina, *ibid.* **147**, 423 (1966).

[4]P. G. de Gennes, Solid State Commun. **1**, 132 (1963).

[5]M. Tokunaga and T. Matsubara, Prog. Theor. Phys. **35**, 581 (1966); **36**, 857 (1966).

[6]R. Blinc, P. Prelovšek, Solid State Commun. **42**, 893 (1982).

[7]R. Blinc, J. Bjorkstam, Phys. Rev. Lett. **23**, 788 (1969).

[8]J. L. Bjorkstam, Adv. Magn. Res. **7**, 1 (1974).

[9]G. J. Adriaenssens, Phys. Rev. B **12**, 5116 (1975).

[10]M. Mali, J. Roos, E. Courtens, and K. A. Müller, *Proceedings of the 22nd Congress Ampere, Zurich, 1984,* edited by K. A. Müller, R. Kind, and J. Roos (University of Zurich, Zurich, 1984), p. 32.

[11]M. Mali, J. Roos, E. Courtens, and K. A. Müller, Ferroelectrics **53**, 215 (1984).

[12]E. Courtens, Phys. Rev. Lett. **39**, 56 (1977); **41**, 1171 (1978).

[13]A. S. Chaves and R. Blinc, Phys. Rev. Lett. **43**, 1037 (1979).

[14]T. Takoshima, I. Tatsuzaki, T. Hikita, J. Phys. Soc. Jpn. **37**, 574 (1974); **39**, 431 (1975); A. P. Zhukov, I. S. Rez, V. I. Pakhomov, and A. G. Semin, Phys. Status Solidi **27**, K129 (1968).

[15]R. Blinc, J. Slak, B. Ložar, and S. Žumer, preceding paper, Phys. Rev. B **34**, 3108 (1986).

[16]R. Blinc, M. Mali, J. Slak, J. Stepišnik, and S. Žumer, J. Chem. Phys. **56**, 3566 (1972); G. Bonera, F. Borsa, M. L. Crippa, and A. Rigamonti, Phys. Rev. B **4**, 52 (1971).

[17]G. L. Paul, W. Cochran, W. J. L. Buyers, and R. A. Cowley, Phys. Rev. B **2**, 4603 (1970).

[18]R. Blinc, M. Mali, J. Pirš, and S. Žumer, J. Chem. Phys. **58**, 2262 (1978); R. Blinc, M. Mali, R. Osredkar, R. Parker, J. Seliger, and S. Žumer, J. Chem. Phys. **59**, 2947 (1973).

[19]C. Filipič and A. Levstik, Fizika, Suppl. **8**, 232 (1976).

[20]G. J. Adriaenssens and J. L. Bjorkstam, Phys. Status Solidi (A) **18**, 129 (1973).